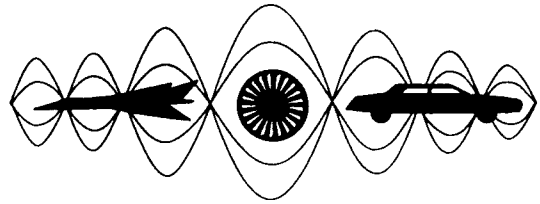

FIFTH INTERNATIONAL CONGRESS ON SOUND AND VIBRATION
DECEMBER 15-18, 1997
ADELAIDE, SOUTH AUSTRALIA

# METHODS FOR COMPUTING THE PASSIVE WIDEBAND CROSS-AMBIGUITY FUNCTION

Kam W. Lo and Brian G. Ferguson
Defence Science and Technology Organisation
P.O. Box 44 Pyrmont NSW Australia

## ABSTRACT

For a fast moving acoustic source in proximity to a pair of widely spaced sensors, the conventional cross correlation method results in poor time delay estimates because the signal received by each sensor experiences a different degree of time scaling. The correct procedure for time delay estimation in this case is to match the time scales of the two received signals, prior to cross correlating them. In practice, the relative time scale between the two signals is not known *a priori* and hence it must be estimated jointly with the time delay. This can be done by evaluating the passive wideband cross-ambiguity function. Four different methods are described for computing this function. The most efficient method is applied to synthetic acoustic data which simulate the outputs of three widely spaced microphones during the low altitude transit of a jet aircraft. The resulting time delay estimates are used to calculate the angular trajectory of the aircraft during the transit.

## 1. INTRODUCTION

The differential time of arrival of an acoustic signal at two spatially-separated sensors can be estimated by cross correlating the sensor outputs [1]. However, when a signal source undergoes fast motion in proximity to a pair of widely spaced sensors, the estimate of the differential time of arrival (often simply called time delay) is in error because the time scale of the received signal is different for each sensor [2-3]. Time scaling, which corresponds to compression or expansion of the signal's time base, is a manifestation of the Doppler effect and so, when a moving source approaches or recedes from a stationary sensor, the received signal appears to be a time compressed or expanded version of the emitted signal. Though the effect of relative time scaling (often referred to as differential Doppler) may be reduced by using a smaller integration (or observation) time for the cross correlator, in many cases, this simple expedient results in an unacceptable reduction in processing gain and hence poor time delay estimates. The correct procedure for time delay estimation in the presence of differential

Doppler is to match the time bases of the two received signal waveforms (for instance, by expanding the time base of the more compressed waveform), prior to cross-correlating them. Since the relative time scale between the received signals is not known *a priori*, it must be estimated, along with the time delay.

This paper considers the use of the passive wideband cross-ambiguity function for the joint estimation of the relative time scale and time delay. Four different methods are described for computing this function. The most efficient method is applied to synthetic acoustic data which simulate the outputs of three widely spaced microphones during the low altitude transit of a jet aircraft. The resulting time delay estimates are used to calculate the variation with time of the azimuth and elevation angles of the aircraft during the transit.

## 2. SIGNAL MODEL

For a moving source, the outputs of a pair of stationary sensors, labelled 1 and $m$, can be represented *locally* over a short time interval $\delta$ by [4]

$$y_1(t) = s(t) + n_1(t) \qquad \text{for } |t| < \delta \tag{1}$$

$$y_m(t) = \rho_{21}\, s\left(\frac{t-\beta_{m1}}{\alpha_{m1}}\right) + n_m(t) \qquad \text{for } |t-\beta_{m1}| < \delta \tag{2}$$

where $s(t)$ is a broadband signal emitted from the source, $n_1(t)$ and $n_m(t)$ are additive noises for the respective sensors, $\alpha_{m1}$ and $\beta_{m1}$ are the relative time scale and time delay between the two sensors respectively, and $\rho_{m1}$ is an attentuation factor. It is assumed that $s(t)$, $n_1(t)$ and $n_m(t)$ are stationary and mutually uncorrelated.

Note that Eqs. (1) and (2) are valid for different time intervals which may or may not be (partially) overlapped depending on the actual source-sensor geometry. This has important implications on the processing requirement. When $\beta_{m1}$ is small compared with $\delta$, the joint estimation of $\alpha_{m1}$ and $\beta_{m1}$ simply requires observing the outputs of the two sensors over the same period of time $[-T_1/2, T_1/2]$, where $\beta_{21} \ll T_1/2 < \delta$. This is the case that has been considered in the open literature. However, when the spacing between the two sensors is very large, it is likely that $\beta_{m1} > \delta$, especially when the signal is emitted from the source near the endfire direction. In this case, the joint estimation of $\alpha_{m1}$ and $\beta_{m1}$ requires the observation time interval for sensor $m$, $[-T_m/2, T_m/2]$, to be sufficiently larger than that for sensor 1, $[-T_1/2, T_1/2]$, so that the signal given by Eq. (2) is included in the observation. The upper bound on the extra observation time required for sensor 2 is simply *twice* the maximum time delay between the two sensors, that is, $2\max\{\beta_{m1}\} = 2d_{m1}/c$, where $d_{m1}$ is the sensor spacing and $c$ is the speed of sound.

## 3. PASSIVE WIDEBAND CROSS-AMBIGUITY FUNCTION

The relative time scale and time delay $\alpha_{m1}$ and $\beta_{m1}$ are estimated jointly by evaluating the passive wideband cross-ambiguity function defined by

$$A_{y_m y_1}(\tau, \sigma') = \sqrt{\sigma'} \int_{-\infty}^{\infty} y_m(t)\, y_1^*[\sigma'(t-\tau)]\, dt, \quad \sigma' > 0 \tag{3}$$

where $\tau$ and $\sigma'$ are the time delay and time scales variables respectively, and $*$ denotes complex conjugation. Under the change of variables $\sigma' \rightarrow 1/\sigma$, the passive wideband cross-

ambiguity function is equivalent to the continuous wavelet transform of $y_m(t)$ with respect to the mother wavelet $y_1(t)$, that is

$$W_{y_1 y_m}(\tau,\sigma) = \frac{1}{\sqrt{\sigma}} \int_{-\infty}^{\infty} y_m(t)\, y_1^*\left(\frac{t-\tau}{\sigma}\right) dt\,, \quad \sigma > 0\,. \tag{4}$$

The limits of the continuous wavelet transform's integral are from -∞ to ∞, but for the present application, $y_m(t)$ and $y_1(t)$ are essentially time-limited to $[-T_m/2, T_m/2]$ and $[-T_1/2, T_1/2]$ respectively, where $T_m = T_1 + 2d_{m1}/c$. Thus, the practical implication of employing Eq. (4) is that it will be applied to two signals with different durations and needs to be computed only during the time period $[-\sigma T_1/2 + \tau,\ \sigma T_1/2 + \tau]$. The finite observation time $T_1$ is bounded above by $2\delta$, which ensures the signal model is valid. It is bounded below by the condition [3] that the correlation times of the signal and noise are much less than $T_1$ so that the time correlation $W_{y_1 y_m}(\tau,\sigma)/(\sqrt{\sigma}\, T_1)$ gives a useful approximation to the ensemble average over the noise and signal distributions when $\sigma$ matches the relative time scale $\alpha_{m1}$.

In practice, $W_{y_1 y_m}(\tau,\sigma)$ is evaluated at discrete values of $\tau$ and $\sigma$ using samples of $y_1(t)$ and $y_m(t)$ as follows:

$$W_{y_1 y_m}(qT_s, \sigma_p) \approx \frac{1}{f_s\sqrt{\sigma_p}} \sum_k y_m(kT_s)\, y_1^*\left(\frac{k-q}{\sigma_p} T_s\right), \quad \sigma_p > 0 \tag{5}$$

where $p$, $q$, $k$ are integers, $f_s$ is the sampling frequency and $T_s = 1/f_s$. The estimates of $\beta_{m1}$ and $\alpha_{m1}$ are given respectively by the values of $qT_s$ and $\sigma_p$ that maximise $W_{y_1 y_m}(qT_s, \sigma_p)$. A two-dimensional grid search is performed to obtain the global maximum .

## 4. COMPUTATION METHODS

### 4.1. MULTIRATE SAMPLING

The time-scaled replicas $y_1(kT_s/\sigma_p)$ can be created from $y_1(kT_s)$ using the multirate sampling method [5]. The time scale value $\sigma_p$ is written as $I/D$, where $I$ and $D$ are positive integers. To change the sampling rate of the signal from $f_s$ to $\sigma_p f_s$, the sampling rate is first increased to $If_s$ by adding $(I\text{-}1)$ zeros between each pair of signal samples $\{y_1(kT_s), y_1[(k+1)T_s]\}$, then the resultant signal is passed through a low pass filter for anti-imaging and antialiasing, and finally every $D$th sample of the filter output is selected. To improve the computational efficiency, multistaging [5] is often used. This requires decomposing $I$ and $D$ into products of prime numbers and using multiple lower order low pass filters.

For a given time scale value $\sigma_p$, Eq. (5) indicates that $W_{y_1 y_m}(qT_s, \sigma_p)$ is a discrete (linear) correlation of $y_m(kT_s)$ and $y_1(kT_s/\sigma_p)$, which can be computed using the fast Fourier transform as follows. Assume $y_1(kT_s)$ has a length of $L_1$ ($-L_1/2 \le k \le L_1/2\text{-}1$) and $y_m(kT_s)$ has a length of $L_m$ ($-L_m/2 \le k \le L_m/2\text{-}1$), where $L_1$, $L_m$ are even and $L_1 < L_m$. The length of the fast Fourier transform, $M$, is chosen to avoid circular correlation, that is, $M$ is a power of 2 such that $M \ge L_2 + L_1 \max\{\sigma_p\} - 1$. The sequences $y_m(kT_s)$ and $y_1(kT_s/\sigma_p)$ are first padded to the same length $M$ with the appropriate numbers of zeros. Then the fast Fourier transform of

$y_m(kT_s)$ is multiplied by the complex conjugate of the fast Fourier transform of $y_1(kT_s/\sigma_p)$. Finally, the inverse fast Fourier transform of the resulting product is divided by $f_s\sqrt{\sigma_p}$.

## 4.2. DISCRETE FOURIER TRANSFORM INTERPOLATION

A simpler way to create time-scaled replicas $y_1(kT_s/\sigma_p)$ is to interpolate $y_1(kT_s)$ using the *discrete* Fourier transform which does not require any low pass filter. In this method, the time scale values are limited to $\sigma_p = (L_1 + p)/L_1$, where $L_1$ is the length of the sequence $y_1(kT_s)$ and $p$ is an integer multiple of 2. Let $Y_1(k)$ be the discrete Fourier transform of $y_1(kT_s)$, $-L_1/2 \le k \le L_1/2 - 1$.

(a) Time base expansion (dilation)

For $\sigma_p > 1$ ($p > 0$), $p/2$ zeros are appended to each end of $Y_1(k)$, which effectively increases the sampling rate from $f_s$ to $\sigma_p f_s$. Taking the inverse discrete Fourier transform of the zero-padded spectrum and multiplying the result by $\sigma_p$ gives $y_1(kT_s/\sigma_p)$, $-(L_1 + p)/2 \le k \le (L_1 + p)/2 - 1$.

(b) Time base compression (contraction)

To avoid aliasing, the new sampling frequency $\sigma_p f_s$ must be at least twice the signal bandwidth $B_1$, that is, $\sigma_p f_s \ge 2B_1$, and this places a lower bound on $\sigma_p$. For example, if $f_s = 4B_1$, the lower bound on $\sigma_p$ will be 1/2, which is good enough for most applications as the relative time scale is seldom less than 1/2. For $1/2 < \sigma_p < 1$ $(-L_1/2 < p < 0)$, $L_1/2 + p$ zeros are appended to each end of $Y_1(k)$, which effectively increases the sampling rate to $2\sigma_p f_s$. Taking the inverse discrete Fourier transform of the zero-padded spectrum and multiplying the result by $2\sigma_p$ yields $y_1(kT_s/2\sigma_p)$, $-(L_1 + p) \le k \le (L_1 + p) - 1$. Retaining one for every two samples of $y_1(kT_s/2\sigma_p)$ gives $y_1(kT_s/\sigma_p)$, $-(L_1 + p)/2 \le k \le (L_1 + p)/2 - 1$, with the sampling rate of $y_1(t)$ now effectively being $\sigma_p f_s$.

Having obtained the time-scaled replicas $y_1(kT_s/\sigma_p)$, $W_{y_1 y_m}(qT_s, \sigma_p)$ is computed for each value of $\sigma_p$ using fast correlation via the fast Fourier transform.

## 4.3. CHIRP-Z TRANSFORM

Using Parseval's theorem, Eq. (4) can be written as

$$W_{y_1 y_m}(\tau, \sigma) = \sqrt{\sigma} \int_{-\infty}^{\infty} Y_m(f) Y_1^*(\sigma f) e^{j2\pi f\tau}\, df\,, \quad \sigma > 0 \tag{6}$$

where $Y_n(f)$ is the Fourier transform of $y_n(t)$ for $n = 1, m$. Evaluating Eq. (6) at discrete values of $\tau = qT_s$ and $\sigma = \sigma_p > 0$, and approximating the integral with a finite summation gives

$$W_{y_1 y_m}(qT_s, \sigma_p) \approx \frac{\sqrt{\sigma_p}}{f_s M} \sum_{k=-M/2}^{M/2-1} Y_{dm}(kf_s/M)\, Y_{d1}^*(\sigma_p k f_s/M)\, e^{j2\pi qk/M} \tag{7}$$

where $Y_{dn}(kf_s/M)$ are the samples of the discrete-time Fourier transform of $y_n(t)$ defined by

$$Y_{dn}(f) = \sum_k y_n(kT_s)\, e^{-j2\pi kfT_s}. \tag{8}$$

In Eq. (7), $M \geq L_m + L_1 \max\{\sigma_p\} - 1$ is chosen to implement the linear correlation indicated in Eq. (4) rather than a circular correlation; usually, $M$ is chosen to be a power of 2. Given $Y_{dm}(kf_s/M)$ and $Y_{d1}^*(\sigma_p kf_s/M)$, Eq. (7) can be computed efficiently using an inverse $M$-point fast Fourier transform.

$Y_{dm}(kf_s/M)$ is obtained by padding each end of $y_m(kT_s)$ with $(M\text{-}L_m)/2$ zeros, followed by an $M$-point fast Fourier transform. The scaled wavelet spectrum, $Y_{d1}(\sigma_p kf_s/M)$, is computed using the chirp z-transform as suggested in Reference [6]. The computation time of the chirp z-transform is only a few times longer than that of an $M$-point fast Fourier transform.

### 4.4. CROSS-WAVELET TRANSFORM

$W_{y_1 y_m}(\tau,\sigma)$ can also be evaluated using the cross-wavelet transform [5], that is,

$$W_{y_1 y_m}(\tau,\sigma) = \frac{1}{c_g}\int_{-\infty}^{\infty}\int_{-\infty}^{\infty} W_g y_m(b,a)\, W_g^* y_1\left(\frac{b-\tau}{\sigma}, \frac{a}{\sigma}\right)\frac{dadb}{a^2}, \quad \sigma > 0 \tag{9}$$

where $W_g y_n(b,a)$ is the continuous wavelet transform of $y_n(t)$ with respect to an arbitrarily chosen mother wavelet $g(t)$ ($n$ = 1,$m$) and $c_g$ is the admissibility constant. The continuous wavelet transform of $W_g y_n(b,a)$ is defined by

$$W_g y_n(b,a) = \frac{1}{\sqrt{|a|}}\int_{-\infty}^{\infty} y_n(t)\, g^*\left(\frac{t-b}{a}\right)dt \tag{10}$$

where $a$ and $b$ are the time scale and time delay variables respectively, and both $a$ and $b$ can be positive or negative. Usually, the mother wavelet $g(t)$ is complex so that the resulting continuous wavelet transform, $W_g y_n(b,a)$, is also complex. If $g(t)$ has a real spectrum, then for real signals $y_1(t)$ and $y_m(t)$, it can be shown that Eq. (9) can be written as

$$W_{y_1 y_m}(\tau,\sigma) = \frac{2}{c_g}\mathrm{Re}\left[\int_0^{\infty}\frac{da}{a^2}\int_{-\infty}^{\infty} W_g y_m(b,a)\, W_g^* y_1\left(\frac{b-\tau}{\sigma}, \frac{a}{\sigma}\right)db\right], \quad \sigma > 0 \tag{11}$$

where Re[ ] denotes the real part of the bracketed quantity. Eq. (11) can be evaluated at discrete values of $\tau = qT_s$ and $\sigma = \sigma_p > 0$ by approximating the double integral with a finite double summation. It is clear that a two dimensional interpolation is required (to obtain the second term of the double summation) for every value of $\sigma_p$.

### 4.5. COMPARISON OF DIFFERENT METHODS

In the multirate sampling method, the time scale values $\sigma_p$ are of the form $I/D$. The crucial issue of this approach is the design of the multistage low pass filters. Efficiency can be improved by optimizing the order of the filter at each stage. However, if a fine time-scale increment is required, the interpolation factor $I$ and decimation factor $D$ will be quite large, and consequently, many filters are needed. This is often impractical. In addition, creating each of the replicas $y_1(kT_s/\sigma_p)$ requires a new set of filters. Consequently, this method is computationally intensive even for moderate time-scale increments. Another problem with

this method is that the low pass filters will introduce time delays to each replica $y_1(kT_s/\sigma_p)$, and these must be compensated for when estimating the differential time of arrival.

With the discrete Fourier transform interpolation method, the values of $\sigma_p$ are limited to $(L_1+p)/L_1 \geq 2B_1/f_s$. A smaller time-scale increment requires a longer sequence of $y_1(kT_s)$, that is, a larger $L_1$. However, the largest value of $L_1$ is limited by the sampling frequency and the maximum observation time over which the signal model remains valid. Though this problem may be overcome by padding $y_1(kT_s)$ with zeros to increase the effective signal length, the cost of computing the discrete Fourier transform increases with $L_1$. Therefore, this method becomes less efficient for very fine time-scale increments ($\leq 10^{-4}$). Nevertheless, for time-scale increments on the order of $10^{-3}$, or larger, this method is the most efficient.

The main advantage of the chirp z-transform method over the previous two methods is that the time scale values $\sigma_p$ are arbitrary and so very fine time-scale increments can be achieved without increasing the system complexity or the signal length. The efficiency of this method relies on the computational cost of the $M$-point chirp z-transform which is only a few times larger than that of an $M$-point fast Fourier transform. Consequently, for time-scale increments of the order of $10^{-3}$, or larger, this method is less efficient than the discrete Fourier interpolation method but it is more efficient than the others.

With the cross-wavelet transform method, the processing is performed in the wavelet domain. Although this method bypasses the need for multirate sampling, it is computationally very intensive as a two dimensional interpolation is required for every time scale value $\sigma_p$.

To conclude, the discrete Fourier transform interpolation method is the most efficient method to compute the passive wideband cross-ambiguity function for the joint estimation of relative time scale and time delay unless the required time-scale increment is too fine ($\leq 10^{-4}$), in which case the chirp z-transform method is recommended.

## 5. COMPUTER SIMULATIONS

A series of computer simulations were carried out to study the joint estimation of the relative time scale and time delay using the passive wideband cross-ambiguity function. The discrete Fourier transform interpolation method, chirp z-transform method, and cross-wavelet transform method were each used to compute the function for a variety of signal-to-noise ratio scenarios, for both small and large time delays, and for various relative time scales. In each case, the same results were obtained for all three methods. Assessing the computation time for each method used in the simulation verified that the discrete Fourier transform interpolation method was the most efficient for the given time scale resolution, followed by the chirp z-transform method. Moreover, the cross-wavelet transform method was found to be so computationally intensive that it was considered unsuitable for practical applications.

### 5.1. ANGULAR LOCATION OF JET AIRCRAFT

Synthetic acoustic data were generated, which simulate the outputs of three sensors (microphones) during the low altitude transit of a jet aircraft. The three sensors, labelled 1, 2 and 3, were located on the $x$-$y$ plane at (0,0), (-25m,0) and (0,-25m) respectively. The jet was in level flight with a velocity of 300 knots parallel to the -$y$ axis. It experiences a closest point of approach to sensor 1 at a range of 1000 feet, and the signal emitted from the jet at this time instant arrived at the output of sensor 1 with a signal-to-noise ratio of 0 dB. The sampling frequency is $f_s$ = 2 kHz and the speed of sound in air is $c$ = 340 m/s. The data were divided

into overlapped blocks and then processed so as to produce 25 observations per second, with the frequency range of interest being 100-300 Hz. The length of each data block (observation time) is $T_1 = 0.34$ s for sensor 1 and $T_m = 0.487$s for other sensors.

The data were first processed using the conventional cross correlation method. Since the relative time scale between sensors 1 and 2 was close to unity, good time delay estimates were obtained for this pair of sensors. On the other hand, the time delay estimates for sensors 1 and 3 were poor because their relative time scale differed significantly from unity.

The same data set was then processed by evaluating the passive wideband cross-ambiguity function using the discrete Fourier transform interpolation method. The time-scale increment is about 0.0088. Good time delay estimates were obtained for both pairs of sensors (1,2) and (1,3). Figures 1 and 2 show the estimates of the time delay and relative time scale between sensors 1 and 3, together with the actual values, as a function of time respectively. The time delay estimates for both pairs of sensors were used to calculate the variation with time of the elevation and azimuth angles of the aircraft using a far-field approximation, and the results are shown in Figure 3 and 4 respectively. The discrepancy between the actual and estimated angular trajectories is due to the use of the far-field approximation in angle estimation.

## 6. CONCLUSIONS

For a fast moving acoustic source in proximity to widely spaced sensors, the time delay estimates obtained using the conventional cross-correlation method are poor because the time scale of the received signal is different at each sensor location. Joint estimation of the relative time scale and time delay between two sensors can be accomplished by evaluating the passive wideband cross-ambiguity function (or equivalently, with a change of variables, the continuous wavelet transform). In practical applications requiring time-scale increments of the order of $10^{-3}$, or larger, the discrete Fourier transform interpolation method is the most efficient to compute this function, followed by the chirp-z transform method. Both multirate sampling and cross wavelet transfrom methods are computationally intensive and thus not suitable for practical applications. The use of the passive wideband cross-ambiguity function for the angular location of a jet aircraft during its low altitude transit was demonstrated using synthetic acoustic data.

## 7. REFERENCES

[1] G. C. Carter, "Time-delay estimation for passive sonar processing," *IEEE Trans.*, **ASSP-29** (3), 1981, pp.463-470.

[2] W. R. Remley, "Correlation of signals having a linear delay," *JASA* **35** (1), 1963, pp.65-69.

[3] W. B. Adams, J. P. Kuhn, and W. P. Whyland, "Correlator compensation requirements for passive time-delay estimation with moving source or receivers," *IEEE Trans.*, **ASSP-28** (2), 1980, pp.158-168.

[4] Ferguson, B.G. and Lo, K.W., "Passive wideband cross-correlation with different Doppler compensation using the continuous wavelet transform", submitted for publication to *JASA*.

[5] L. G. Weiss, "Wavelets and wideband correlation processing," *IEEE Signal Process. Mag.*, Jan. 1994, pp.13-32.

[6] Jones, D.L. and Baraniuk, R.G., "Efficient Approximation of Continuous Wavelet Transforms", *Electronics Letters*, Vol. 27, No. 9, April 1991, pp. 748-750.

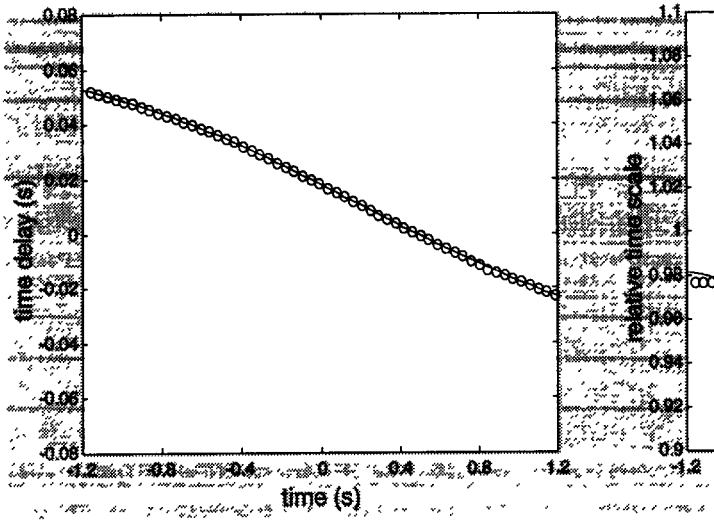


Figure 1:Time delay between sensors 1 and 3. estimate o, actual ——

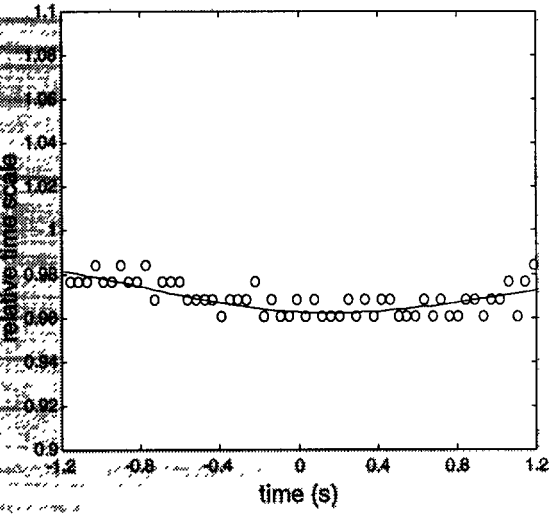


Figure 2:Relative time scale between sensors 1 and 3. estimate o, actual ——

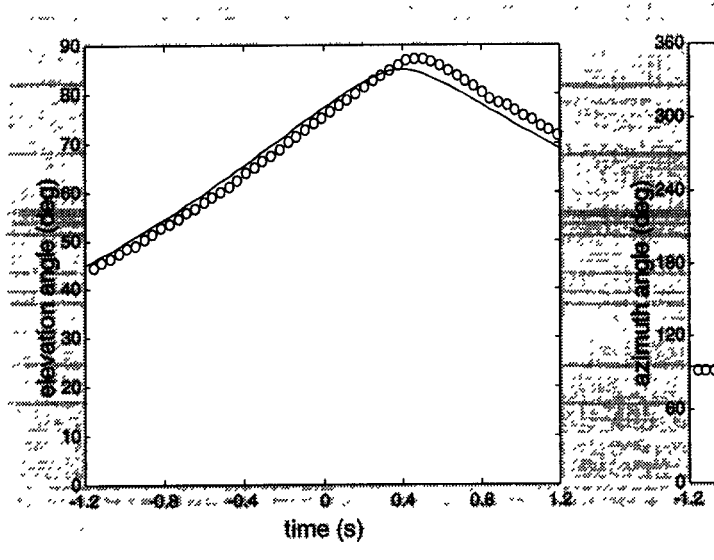


Figure 3:Elevation angle of aircraft. estimate o, actual ——

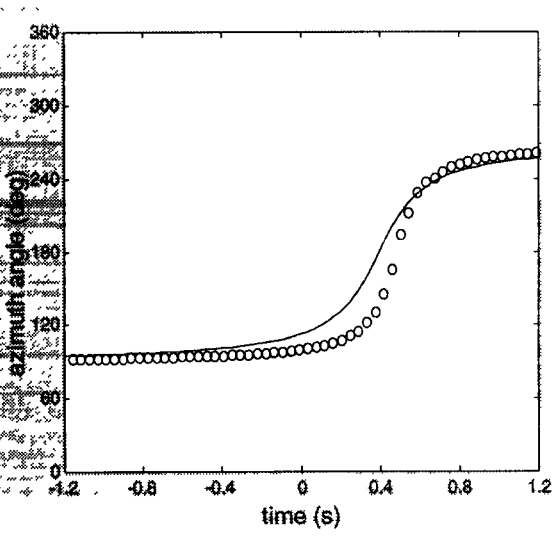


Figure 4:Azimuth angle of aircraft. estimate o, actual ——